PAPER Special Section on Networking Technologies for Mobile Internet Systems

The Reliability Performance of Wireless Sensor Networks Configured by Power-Law and Other Forms of Stochastic Node Placement

Mika ISHIZUKA[†a)] ***and*** **Masaki AIDA**[†b)]**,** ***Members***

SUMMARY Sensor nodes are prone to failure and have limited power capacity, so the evaluation of fault tolerance and the creation of technology for improved tolerance are among the most important issues for wireless sensor networks. The placement of sensor nodes is also important, since this affects the availability of nodes within sensing range of a target in a given location and of routes to the base station. However, there has been little research on the placement of sensor nodes. Furthermore, all research to date has been based on deterministic node placement, which is not suitable when a great many sensor nodes are to be placed over a large area. In such a situation, we require stochastic node placement, where the sensor-positions are in accord with a probability density function. In this paper, we examine how fault tolerance can be improved by stochastic node placement that produces scale-free characteristics, that is, where the degree of the nodes follows a power law.

key words: *sensor network, node placement, fault tolerance, power law*

1. Introduction

Recent advances in electronics, such as power-saving LSIs, have led to the production of small sensors equipped with communications capability. A network of such sensors will enable information gathering over a wide area, so interest in sensor networks is currently strong.

The development of ad hoc network technology is important for wireless-networked sensors, since the ad hoc approach will relieve the network implementor of explicit network configuration. Furthermore, sensor nodes are prone to failure and have limited power capacity, so the evaluation of fault tolerance and the creation of technology for improved tolerance are also major issues for sensor networks. As is the case for ad hoc networks [1], [2], most research on fault tolerance in sensor networks to date has been focused on the power-saving mode of the MAC protocol [3]–[5] and energy-efficient route selection [6]–[8].

Though sophisticated routing and use of the MAC layer protocol will improve fault tolerance, the placement of sensor nodes also strongly affects fault tolerance in a sensor network.

However, little research into placement has been done. In addition, all research to date has been based on deterministic node placement [9]–[11], which requires that each sensor node be placed at predetermined coordinates. This has the following shortcomings:

- a high cost of placement and
- luck of clarity regarding the effects of errors in sensor-position on performance.

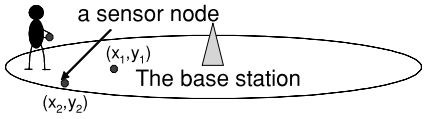

Fig. 1 Concept of deterministic node placement.

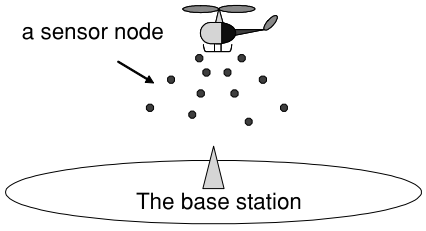

Fig. 2 Concept of stochastic node placement.

The alternative approach is stochastic node placement, where the sensor-positions are determined by a probability density function. Approximate positioning satisfies the density function, so the cost of placement is low. The concepts of the two approaches to placement are shown in Figs. 1 and 2.

Considering the respective characteristics, stochastic node placement is particularly effective when

- the region where sensor nodes are placed is large and outdoors, and has conditions that make precise surveying hard (for example, a big park, a forest, a place where dangers exist), and
- the number of sensor nodes is large.

In order to show effectiveness of stochastic node placement, we should show how to realize stochastic node placement, though this paper focuses only on the evaluation of fault tolerance for stochastic node placement. We consider any stochastic node placement can be realized by scattering sensor nodes from the air (see Fig. 2). The theoretical basis for this consideration is briefly described in Sect. 2.2.

Note that this paper deals with fault tolerance against both random failure and battery exhaustion, although most

Manuscript received January 16, 2003.
Manuscript revised May 27, 2004.

[†]The authors are with the NTT Information Sharing Platform Laboratories, NTT Corporation, Musashino-shi, 180-8585 Japan.
a) E-mail: ishizuka.mika@lab.ntt.co.jp
b) E-mail: aida.masaki@lab.ntt.co.jp

other studies to date have been based on evaluation of the latter point alone. This is because we consider that fault tolerance against random failure is also important, since sensor nodes are prone to failure (e.g. for environmental reasons such as bad weather or because of mechanical trouble). In addition, the evaluation of fault tolerance against random failure is equivalent to evaluation of the effects of changes to the number of sensor nodes. The evaluation of fault tolerance against random failure is thus a meaningful measure of how effectively sensor nodes are placed by different methods of placement.

The topology of the Internet has been shown to have scale-free characteristics; that is, the degree of the nodes has been shown to follow a power law [12]. In addition, recent research has shown that scale-free networks are highly tolerant of random failure, since such networks have more alternative routes [12]. Therefore, it is natural to expect that we can realize a sensor network with high fault tolerance by constructing the network so that the degree of its nodes follows a power law around the base station.

Motivated by the above considerations, we are examining how fault tolerance can be improved by stochastic node placement that produces scale-free characteristics. In this paper, we start by proposing power-law placement, that is, placement so that the degree of the nodes follows a power-law. We then evaluate the relative fault tolerance of power-law placement and the two most typical forms of stochastic placement. Finally, we identify the optimal placement among them.

The rest of this paper is organized as follows. As background material, Sect. 2 covers the communications model and the three forms of stochastic placement. Section 3 describes the conditions used in simulation. Section 4 gives the results of simulation. Section 5 covers the evaluation of optimal placement. Finally, Sect. 6 is a summary.

2. Background

2.1 Communications Model

In this subsection, we use Fig. 3 in explaining how a sensor network senses and transmits data. We consider the situation where the precise location of the target is unknown but the target is known to be in a certain region. Here, we assume that the target is within region D. An example of an application with such conditions is the monitoring of a vehicle in a forest.

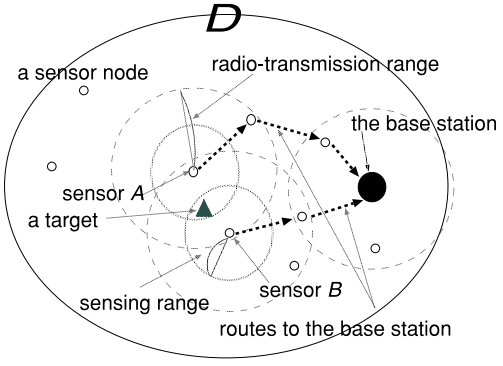

Fig. 3 An example of the sensing and transmission of data.

Each sensor node has a specific sensing range. Each sensor node for which a target is within the sensing range sends sensed information to the base station during each period T. In Fig. 3, sensors A and B are the only sensors capable of sensing the target.

A sensor node can transmit data to or receive data from other sensor nodes within its radio-transmission range. The minimum-hop strategy is used to select routes to the base station. If an intermediate node on the current route breaks down, an alternative route is selected for the remaining information.

Note that we refer to the sensing of a target as successful when one or more sensor nodes is within sensing range of the target, and at least one of these nodes has a route to the base station.

A sensor node consumes battery energy in transmitting (E_t J/bit) and receiving bits (E_r J/bit). When a sensor node used up its battery energy, all functions of the node stop.

2.2 Stochastic Node Placement

In stochastic node placement, sensor-positions $\boldsymbol{x} \in \mathbb{R}^2$ are defined by a probability density function (p.d.f.), $f(\boldsymbol{x})$[†].

In this paper, we evaluate the fault tolerance for three types of stochastic placement. Two are the most typical types, i.e. simple diffusion and constant placement, while the other is our proposal, power-law placement. In this section, we define the p.d.f. of and briefly describe the characteristics of each approach to placement.

We assume that all sensor nodes are placed in region D, which is a circle with radius R. Under this assumption, $\int_D f(\boldsymbol{x})d\boldsymbol{x} = 1$ is required. We set the base station at the center of this circle, and treat this as the origin.

Simple diffusion The simplest way to distribute sensor-nodes is to scatter them from the air above the base station.

Suppose that the weight and shape of the sensor nodes are such that air drag has a strong effect on the way the sensor nodes fall. If air current are weak enough, placement of the sensor nodes will be randomized, so that it follows a diffusion equation. We call this simple diffusion.

Since the solution of a diffusion equation on a two-dimensional boundary is a two-dimensional normal distribution, the p.d.f. of the sensor-positions is

$$f(\boldsymbol{x}) = \frac{C}{2\pi\sigma^2}\, h_0(\|\boldsymbol{x}\|;\sigma), \tag{1a}$$

[†]The probability of a sensor being within region $A = \{x_{11} \le X_1 \le x_{12},\ x_{21} \le X_2 \le x_{22}\}$ can be written in terms of the p.d.f. as follows: $P\{x_{11} \le X_1 \le x_{12},\ x_{21} \le X_2 \le x_{22}\} = \int_{x_{21}}^{x_{22}} \int_{x_{11}}^{x_{12}} f(x_1, x_2)dx_1dx_2$.

where

$$h_0(r,\sigma) \triangleq \exp\left(-\frac{r^2}{2\sigma^2}\right), \text{ and} \tag{1b}$$

$$C = \frac{1}{1-\exp\left(-\frac{R^2}{2}\right)}, \tag{1c}$$

$$0 \le \|\boldsymbol{x}\| \le R.$$

In (1), σ^2 is the variance of the distribution. The variance is determined by several factors (i.e. the shape and weight of the sensors, and the height from which they are released).

Note that sensor nodes scattered from the air are governed by another formula when air currents are strong. However, we do not take such variation into account, since details on techniques for the scattering of sensor nodes are beyond the scope of this paper.

The two-dimensional normal distribution is known as a radial basis function. Daubechies [13] has shown that any functions $F(\boldsymbol{x})$ can be expressed in terms of one or more radial basis functions, as follows:

$$F(\boldsymbol{x}) = \int p(\boldsymbol{c},\sigma)h(\boldsymbol{x};\boldsymbol{c},\sigma)d\boldsymbol{c}d\sigma, \tag{2a}$$

where

$$h(\boldsymbol{x};\boldsymbol{c},\sigma) = \exp\left(-\frac{\|\boldsymbol{x}-\boldsymbol{c}\|}{2\sigma^2}\right). \tag{2b}$$

In (2), $p(\boldsymbol{c},\sigma)$ are weights of each normal distribution, and $\boldsymbol{c}$ and σ^2 are center and variance of the respective normal distributions.

When a radial basis function is used to approximate a given function, the integral in (2) is replaced by a superposition of $h(\boldsymbol{x};\boldsymbol{c}_i,\sigma_i)$ as follows:

$$F(\boldsymbol{x}) \approx \sum_{i=1}^{M} p_i(\boldsymbol{c}_i,\sigma_i)h(\boldsymbol{x};\boldsymbol{c}_i,\sigma_i), \tag{3a}$$

where

$$h(\boldsymbol{x};\boldsymbol{c}_i,\sigma_i) = \exp\left(-\frac{\|\boldsymbol{x}-\boldsymbol{c}_i\|}{2\sigma_i^2}\right). \tag{3b}$$

Also in (3), $p_i(\boldsymbol{c}_i,\sigma_i)$ are weights of each normal distribution, and $\boldsymbol{c}_i$ and σ_i^2 are center and variance of the respective normal distributions. In addition, M is the number of functions being superposed. As for the accuracy of (3), the upper bound of the error has been discussed [14].

Repeated simple diffusion with different centers and variances can thus lead to any form of stochastic sensor-placement. In this sense, simple diffusion is a fundamental distribution in terms of realizing stochastic placement.

Constant placement In much work on sensor networks [5]–[7], [15], placement for uniform probability density of sensor nodes has been assumed. We call this constant placement. In this case, the p.d.f. of sensor-position is as follows:

$$f(\boldsymbol{x}) = \frac{1}{|D|},\ 0 \le \|\boldsymbol{x}\| \le R. \tag{4}$$

In (4), $|D|$ means the area of region D.

Power-law placement (our proposal) The p.d.f. of the sensor-positions in polar-coordinates $f_p(r,\ \theta)$ is

$$f_p(r,\theta) = \frac{\alpha+1}{2\pi R}\left(\frac{r}{R}\right)^{\alpha},$$
$$0 \le r \le R,\ 0 \le \theta < 2\pi, -1 < \alpha < 1. \tag{5}$$

Power-law placement is characterized by the following two features. Firstly, the density of sensor nodes is higher near the base station. Actually, $\rho(r_1,\theta_1)$, the density of sensor nodes at position (r_1,θ_1), is as follows.

$$\begin{aligned}\rho(r_1,\theta_1) &= \lim_{\delta r\to 0}\lim_{\delta\theta\to 0}\frac{\int_{r_1}^{r_1+\delta r}\int_{\theta_1}^{\theta_1+\delta\theta} f(r,\theta)d\theta dr}{\int_{r_1}^{r_1+\delta r}\int_{\theta_1}^{\theta_1+\delta\theta} d\theta dr}\\ &= \frac{\alpha+1}{2\pi}\frac{r_1^{\alpha-1}}{R^{\alpha+1}},\ -2 < \alpha-1 < 0.\end{aligned} \tag{6}$$

Secondly, the degree of the nodes follows a power law. Since a sensor node can transmit data to or receive data from other sensor nodes within the radio-transmission range, the degree of a node may be expressed as the p.d.f. of the number of sensor nodes within radio-transmission range. When the radius of the region D is much larger than the radio-transmission range, the asymptotic behavior of the degree of the nodes is as follows:

$$\begin{aligned}g(x) &= \frac{d}{dx}\int\int_{\rho(r_1,\theta_1)<x} f(r,\theta)drd\theta\\ &= \frac{d}{dx}\int_0^{2\pi}\int_{\frac{1}{2\pi Rx}}^{R}\frac{\alpha+1}{2\pi R}(\frac{r}{R})^{\alpha}drd\theta\\ &\propto x^{\frac{2}{\alpha-1}},\ 2\pi R^2 < x, -1 < \alpha < 1.\end{aligned} \tag{7}$$

From (7), $g(x)$ is proportional to $x^{\frac{2}{\alpha-1}}$, so the degree of the nodes follows a power law.

Here, we briefly give an example of the realization of power-law placement, although we leave details of such realization for further study. As was shown in (3), repeated simple diffusion can be used to produce any stochastic placement. To set masa $\boldsymbol{c_i}$, $(i = 1, \ldots, M)$ to the same position as the base station is one of the simplest parameter settings for (3). In this case, the p.d.f. of placement, $f(\boldsymbol{x})$, is approximated as follows:

$$f(\boldsymbol{x}) \approx \sum_{i=1}^{M}\frac{p_i}{2\pi\sigma_i^2}h_0(\|\boldsymbol{x}\|;\sigma_i). \tag{8}$$

One way to realize (8) is to scatter M types of sensor

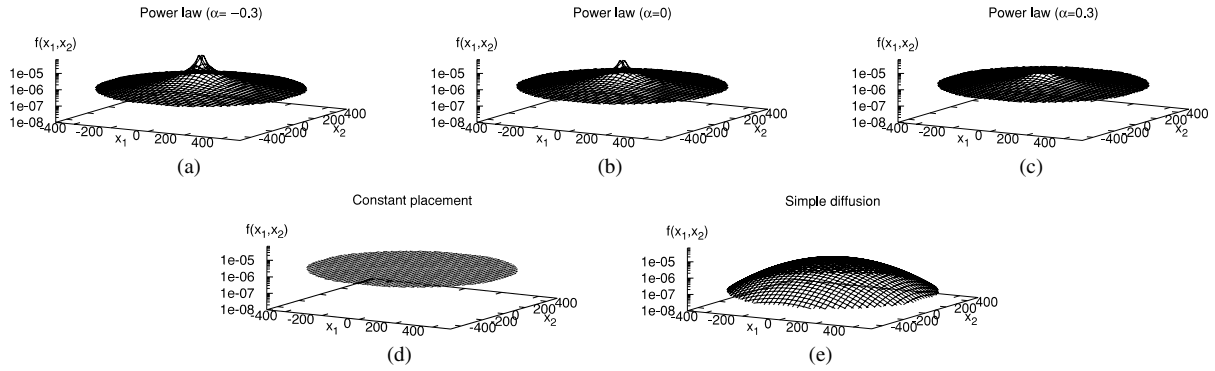

Fig. 4 P.d.f. plots for various placements.

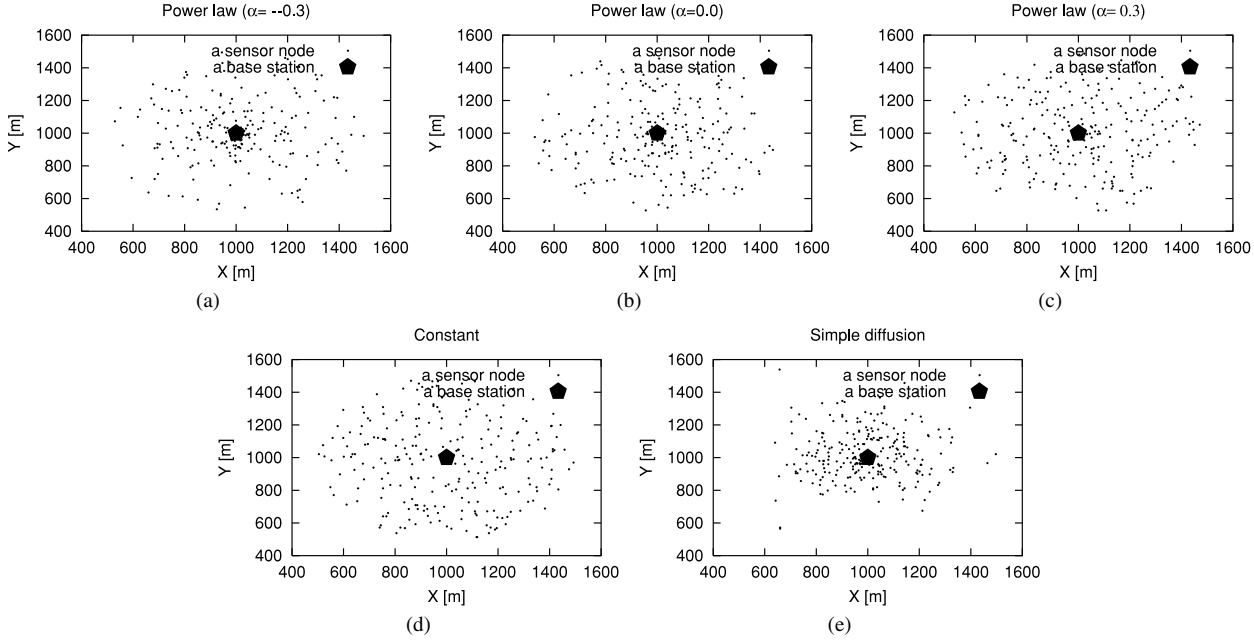

Fig. 5 Examples of various placements.

nodes with different weights (for different σ_i) simultaneously in the air above the base station. The cost of preparing "M" types of sensors with different weights will be low, even if the value of M is great. This is because the M types of sensors can be prepared by merely attaching weights to each sensor. Details on determining the values of M, p_i, and σ_i are not given in this paper, because the focus of this paper is the evaluation of fault tolerance for each placement.

The characteristics of various placements are shown by plots of p.d.f. in Fig. 4 and by examples of placement in Fig. 5. The base station is the origin and region D is a circle with a radius of 500 m, centered on the base station. Variance for simple diffusion is set so that 99% of the sensors are placed within region D. In the other placements, we suppose that all sensor nodes are placed within region D. The number of sensor nodes in Fig. 5 is 250. The density of simple diffusion gradually decreases with distance from the base station and is lowest around the border of region D. The power-law placements also have greatest density near the base station, and this rapidly decreases with distance and then stays almost constant. As α increases, density decreases near the base station and increases around the border of region D.

3. Simulation Settings

3.1 Setting of Targets and Sensor Nodes

Targets were randomly generated within region D, a circle with a radius of 500 m and centered on the base station, covering about seventeen times the area of the Tokyo Dome. We consider that region D is large enough to benefit from the efficiency of stochastic node placement.

In evaluating tolerance of node failures due to battery exhaustion, we set up the target-sensing period, T, to follow an exponential distribution with an average of 72 min. A new target was generated T_I after the end of the target-sensing period for the previous target. We set T_I to follow an exponential distribution with an average of 250 sec.

The number of sensor nodes, N, was 250. We set the sensing range to 60 m and the radio-transmission range to 100 m.

The data transmission rate was 1.1 kbps, low enough to avoid collisions. Actually, the data transmission rate is determined by frequency of sensing and by volume of sensory information. When a certain delay is allowed by an application, frequency of sensing is not so large, since it is reasonable that a sensing node send several times of sensory information collectively. As for volume of sensory information, it is considered to be small. Considering situation where a certain delay is allowed by an application and volume of sensory information is small, we set interval of transmission is 18 min and volume of data to 150 kbytes. Note that, when data transmission rate is high enough that collisions are possible, the collisions affect the rate of battery consumption. In practice, however, we consider these collisions can be avoided by using techniques such as data aggregation [16]. Therefore, our results can apply to the situation where some techniques to avoid collisions are used, though details about such techniques will be considered in further study.

Energy consumption was 3.3e-07 J/bit for transmission and 1.9e-07 J/bit for reception [15]. The initial energy of each sensor node was 20 J.

As was described in Sect. 2.1, target is successfully sensed when the following two conditions are met.

[Condition 1] One or more sensor nodes is within the sensing range of the target, and

[Condition 2] at least one of these nodes has a route to the base station.

Given these simple conditions, simulation parameters need not be changed to investigate the robustness of networks in each placement against failures of nodes. However, the results of quantitative analysis may be affected by the number of sensor nodes in region D and the ratio of sensing range to radio-transmission range.

Therefore, we evaluated two additional cases in determining the best placement (Sect. 5):

- N is changed to 400, and
- N is changed to 400 and sensing range is changed to 30 m.

We evaluated seven forms of power law placement, i.e. $\alpha \in \{-0.5, -0.3, -0.1, 0, 0.1, 0.3, 0.5\}$. In each case, all sensor nodes were placed in region D. This was also the case for constant placement. In the case of simple diffusion, the variance was set so that 99% of sensor nodes would be placed within region D. In evaluating individual items (Sect. 4), sets of five arrangements produced by constant placement, simple diffusion, and power-law placement with three control parameters were evaluated.

3.2 Simulation Scenario

In this subsection, we describe how we evaluated fault tolerance. We considered scenarios where the number of live sensor nodes gradually decreases because of random errors or battery exhaustion.

We adopted the "virtual sensing-success ratio" as the performance metric. This refers to the probability that a given target generated in region D is successfully sensed. This metric is used to evaluate fault tolerance (that is, sensing-success ratio) at arbitrary points in time.

In evaluating tolerance against random failure, we evaluated the virtual sensing-success ratio for various values of r_b, the proportion of broken nodes. We increased r_b from 0 with a step size of 0.1. At each value of r_b, the broken nodes are randomly selected.

In evaluating tolerance against battery exhaustion, we considered a situation where the number of nodes that have used up their battery energy increases with the number of targets. We evaluated the relationship between virtual sensing-success ratio and the number of targets. We also evaluated the total numbers of bits received as a measure of actual (simulated) performance.

4. Results of Simulation

4.1 Tolerance of Random Failure

In the discussion below, 'sensor node' and 'sensor' refer to functioning sensor nodes, except in reference to the original distributions. 'The target' refers to each current target in the sequence.

Results for virtual sensing-success ratio are given in Figs. 6 and 7. In order to examine the results in detail, we plot the probability that no sensor is within sensing range of

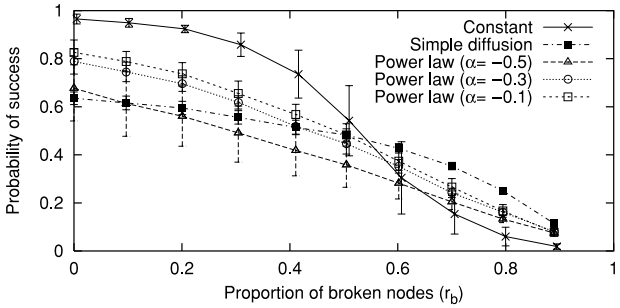

Fig. 6 Virtual sensing-success ratios. ($\alpha = -0.5, -0.3, -0.1$)

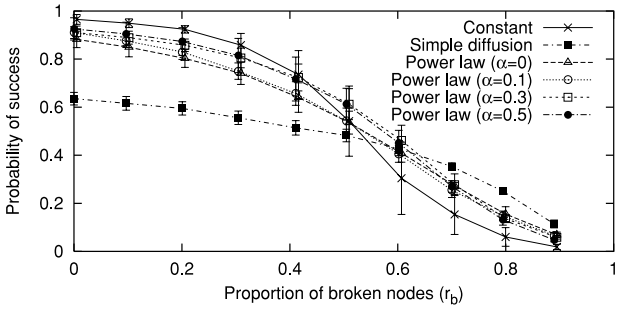

Fig. 7 Virtual sensing-success ratios. ($\alpha = 0, 0.1, 0.3, 0.5$)

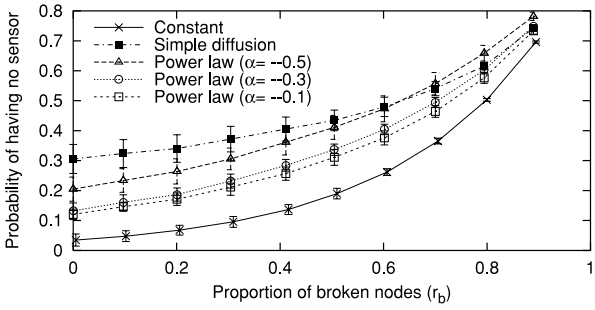

Fig. 8 Probability of having no sensors within range of the target. ($\alpha = -0.5, -0.3, -0.1$)

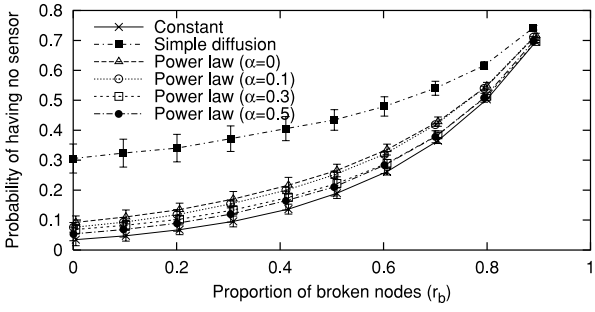

Fig. 9 Probability of having no sensors within range of the target. ($\alpha = 0, 0.1, 0.3, 0.5$)

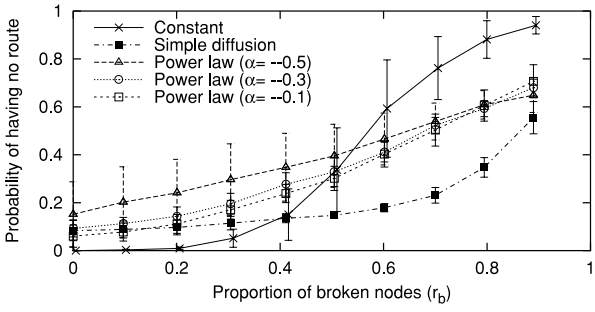

Fig. 10 Probability that no sensor node within sensing range of the target has a route to the base station. ($\alpha = -0.5, -0.3, -0.1$)

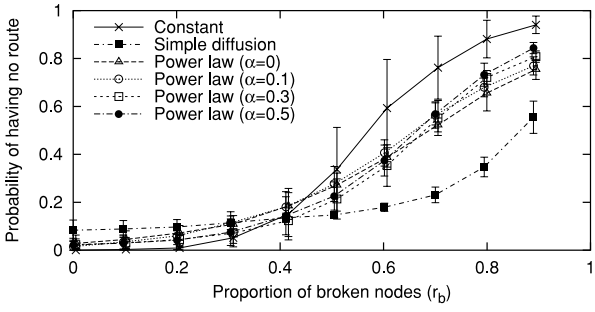

Fig. 11 Probability that no sensor node within sensing range of the target has a route to the base station. ($\alpha = 0, 0.1, 0.3, 0.5$)

the target in Figs. 8 and 9. In addition, the probability that no sensor node within sensing range of the target has a route to the base station in plotted in Figs. 10 and 11 (we call this as the probability of having no route to the base station).

The highest virtual sensing-success ratio is for constant placement when the proportion of broken nodes, r_b, is low. This is because the probability of having no sensor within sensing range of the target is lowest for constant placement (see Figs. 8 and 9). It is obvious that uniform density of sensor nodes is desirable in terms of keeping this probability high. However, the ratio for constant placement drops rapidly after r_b reaches 0.4 and this placement produce the worst result in the region of high r_b. This is because this placement produces the highest probability that there are no routes to the base station when r_b is high (see Figs. 10 and 11). In order to keep the probability that a route to the base station exists high despite random failures, a higher density of sensor nodes near the base station is desirable. This is because sensor nodes near the base station have a higher probability of being used as relay nodes. Since constant placement produces the lowest density of sensor nodes near the base station, the sensing-success ratio for high r_b is lowest.

Simple diffusion has the lowest or second lowest virtual sensing-success ratio when r_b is low, but has the highest ratio when r_b is high. The low sensing-success ratio for simple diffusion in the region of small r_b is because the probability that no sensor is within sensing range of the target is high (see Figs. 8 and 9). This is because simple diffusion produces a distribution with relatively fewer nodes around the border of region D (see Fig. 5). The converse of this characteristic is the relatively higher sensing-success ratio in the region of high r_b. That is, the probability of having no route to the base station is smaller in the region of high r_b (see Figs. 10 and 11) because there are more sensors near the base station.

The virtual sensing-success ratio for the power-law placements increases with α in the region of small r_b. This is mainly because the probability of having no sensor within sensing range of the target decreases with α increases (see Figs. 8 and 9). This decrease in the probability of having no sensor within sensing range of the target is because the density of sensor nodes becomes increasingly uniform as α increases. The differences between the virtual sensing-success ratios for different values of α decrease as r_b increases. This is because the probability of having no route to the base station increases with α in the region of high r_b, while the probability that no sensor is within sensing range of the target decreases as α increases (see Figs. 8–11). The increase is because the density of sensor nodes near the base station decreases with α.

From another point of view, the evaluation of sensing success-ratio when random failure occurs is equivalent to the evaluation of sensing success-ratio when the number of sensor nodes in region D is changed, since the x-axis in Figs. 6 and 7 refrects to the number of live nodes, i.e. $N(1 - r_b)$. We now look at the results in Figs. 6 and 7 from this viewpoint.

The virtual sensing success-ratio for constant placement does not increase greatly when the number of operating nodes increases in the right most region of Figs. 6 and

7. That is, with this distribution, newly added nodes are not effectively placed when the number of sensor nodes is small.

The virtual sensing success-ratio for simple diffusion approaches saturation first and stays relatively low as the number of nodes increases in the left sides of these graphs. In this case, newly added nodes are not effectively placed when the number of sensor nodes is large.

The virtual sensing success-ratio for power-law placement rises linearly with the number of nodes in the right-side and middle regions of these figures. When $\alpha < 0$, this ratio continues to rise linearly in the left-most region of these figures, while the ratios for $\alpha \geq 0$ approach relatively high saturation values in this region. Newly added nodes are thus always effectively placed, regardless of the number of sensor nodes.

4.2 Tolerance of Battery Exhaustion

Relationships between the number of targets that have appeared and the virtual sensing-success ratio are shown in Figs. 12 and 13. To examine these results in more detail, we plot the probability that no sensor is within range of the current target in Figs. 14 and 15, and the probability that no sensor node within sensing range of the target has a route to the base station (that is, the probability of having no route to the base station) in Figs. 16 and 17.

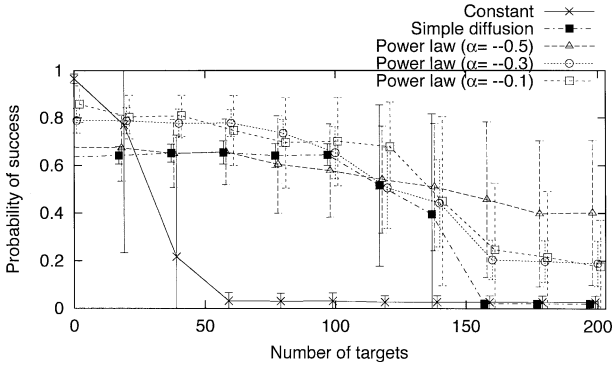

Fig. 12 Virtual sensing-success ratio vs. no. of targets that have appeared. ($\alpha = -0.5, -0.3, -0.1$)

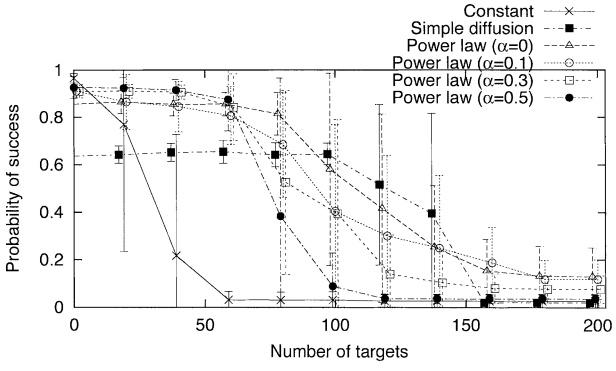

Fig. 13 Virtual sensing-success ratio vs. no. of targets that have appeared. ($\alpha = 0, 0.1, 0.3, 0.5$)

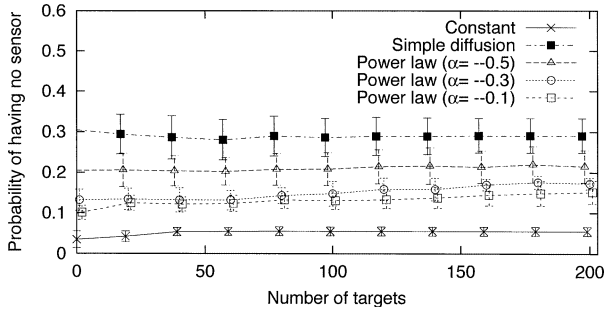

Fig. 14 Probability of having no sensor within range of the target. ($\alpha = -0.5, -0.3, -0.1$)

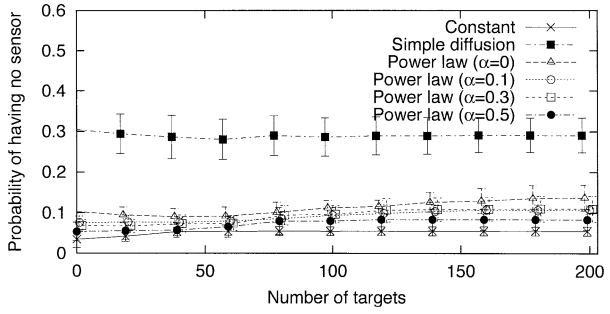

Fig. 15 Probability of having no sensor within range of the targets. ($\alpha = 0, 0.1, 0.3, 0.5$)

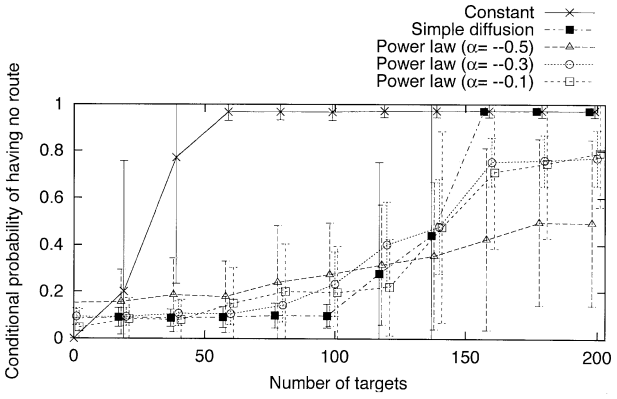

Fig. 16 Probability that no sensor node within sensing range of the target has a route to the base station. ($\alpha = -0.5, -0.3, -0.1$)

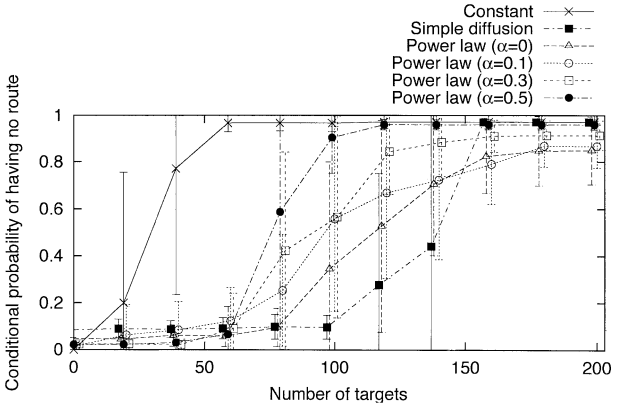

Fig. 17 Probability that no sensor node within sensing range of the target has a route to the base station. ($\alpha = 0, 0.1, 0.3, 0.5$)

The highest virtual sensing-success ratio over simulated time is for constant placement highest when very few targets have appeared. However, the respective plots drop rapidly and are the first to approach 0 (Figs. 12 and 13). This indicates that constant placement is also the weakest approach in terms of failure through battery exhaustion.

While simple diffusion has the lowest ratio when relatively few targets have appeared, the ratios drop and approach zero much more strongly than those for constant placement.

The sensing-success ratios for power-law placement with $\alpha \leq 0$ are almost equal to and generally greater than those for simple diffusion across the whole range. When relatively few targets have appeared in these cases, the virtual sensing-success ratios decrease with α. On the other hand, the period over which the virtual sensing-success ratio stays at a reasonable value becomes longer as α decreases.

These results can be explained as follows. Wile the probability of having no sensors within range of the target determines the virtual sensing-success ratio when relatively few targets have appeared, the probability of having no routes to the base station becomes dominant when relatively many targets have appeared. In a similar way to tolerance of random failure, there is a trade-off between the probabilities of having no sensor within sensing range of the targets and of having no route to the base station. That is, uniform placement of the sensor nodes maximizes the former probability but placement with a high density near the base station is desirable in terms of raising the latter probability.

From these observations, we can say that placement for a uniform density of sensor nodes shows the highest virtual sensing success-ratio when the number of targets is small, while placement for a higher density near the base station keeps the virtual sensing-success ratio at reasonable values over longer periods.

Unlike the characteristics of tolerance of random failure, however, rapid decreases in the virtual sensing-success ratio are seen with most placements. This is because of the rapid increase in the probability of having no route to the base station (Figs. 16 and 17) and the almost constant probability of having no sensor within sensing range of the target (Figs. 14 and 15).

The mechanism behind the rapid increase is as follows. Since sensor nodes near the base station are more likely to be used as relay nodes, their batteries are more rapidly used up. Once some sensor nodes near the base station have used up their batteries, the remaining sensor nodes near the base station are more likely to be used as relay nodes, this situation accelerates the consumption of battery energy by these sensor nodes. Consequently, as the number of targets (simulated time) increases, the density of sensor nodes near the base station more rapidly decreases, although this effect is diminished with distance from the base station. This explains the rapid increase in the probability of having no route to the base station in Figs. 16 and 17.

Considering this acceleration of battery consumption, we conclude that the density of sensor nodes near the base station has a stronger effect on tolerance of battery exhaustion than on tolerance of random failure.

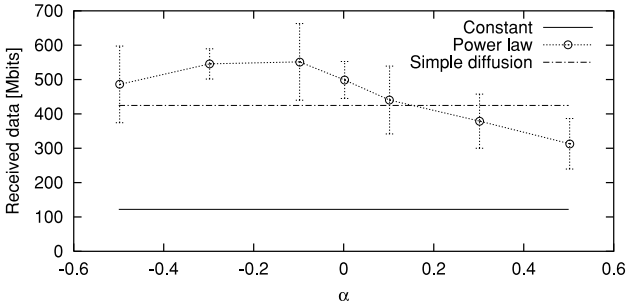

Fig. 18 Total number of received bits.

Finally, the total number of bits actually received by the base station in the above situation is plotted in Fig. 18. Fewer bits are received with constant placement and simple diffusion than with power-law placement when $-0.3 \leq \alpha \leq 0$. In the case of constant placement, a greater probability that there is no route to the base station reduces the cumulative number of bits received. In the case of simple diffusion, a greater probability of having no sensor within range of targets has a similar but weaker effect. In the case of power-law placement, intermediate values of α are desirable in terms of keeping the total number of bits received high, because a smaller value of α raises the probability of having no sensor within range of targets and a larger value of α raises the probability of having no route to the base station. Since these two probabilities are relatively balanced for power-law placements in the range $-0.3 \leq \alpha \leq 0$, relatively higher total numbers of bits are received in this range of Fig. 18.

5. Optimization of Power Law Placement

The simulation-based results in Sect. 4 showed that fault tolerance becomes high when the probabilities of having sensor nodes within range of the targets and of having alternative routes to the base station are both high. Since the former more strongly affects tolerance of random failure while the latter more strongly affects tolerance of battery exhaustion, the most desirable placement differs with the mix of failure types. However, the results of simulation also suggested that we can balance tolerance of the two types of failure by selecting power-law placement with an appropriate value of α. We thus briefly investigate the optimization of power-law placement in this section.

To optimize power-law placement, we need to express a performance metric for each type of failure as a function of α. For tolerance of random failure, we use the expectation of the virtual sensing-success ratio, and for tolerance of battery exhaustion, we use the total number of received bits.

A value of α that maximizes both is most desirable. However, each metric is likely to be maximized by different values of α. We thus suggest the value of α that maximizes

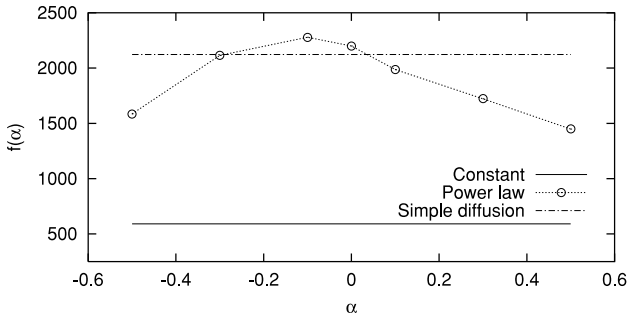

Fig. 19 Plot of $S(\alpha)\,C_r(\alpha)$.

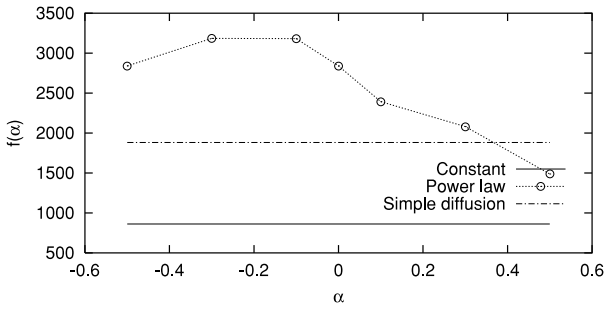

Fig. 20 Plot of $S(\alpha)C_r(\alpha)$. ($N = 400$)

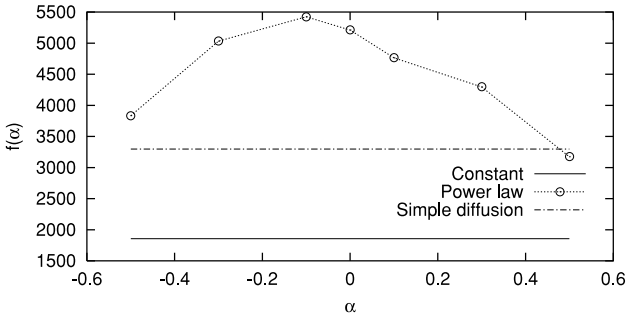

Fig. 21 Plot of $S(\alpha)C_r(\alpha)$. ($N = 400$, sensing range = 30 m)

the product of the two metrics as a suitable optimal value.

We do this with a limited range of α as follows:

$$\max_{\alpha\in\{-0.5,-0.3,-0.1,0,0.1,0.3,0.5\}} S(\alpha)\,C_r(\alpha) \tag{9a}$$

$$\text{where} \qquad S(\alpha) = \sum_{n=0}^{N} S_n P[N_b = n]. \tag{9b}$$

The function $S(\alpha)$ in (9a) is the expectation of the virtual sensing-success ratio when random failure occurs, and is calculated by using (9b). Notation in (9b) is defined as follows:

- N: number of sensor nodes.
- S_n: virtual sensing-success ratio when the number of broken nodes is n (that is, the results in Figs. 6 and 7).
- N_b: the number of broken nodes.

The $C_r(\alpha)$ in (9a) is defined as the total number of received bits when failure through battery exhaustion is occurring (that is, the result in Fig. 18).

In (9a), $S(\alpha)$ is the expectation of the probability that sensing is successful and $C_r(\alpha)$ is proportional to the probability that data is successfully received, which means both metrics do not exceed 1. Therefore, α that makes one metric too large cannot be chosen as the optimal value, even though product of $S(\alpha)$ and $C_r(\alpha)$ is chosen as an objective function.

Suppose that the process of sensors breaking down follows a Bernoulli distribution and that the probability of breakdown, p_b, is 0.001. Under this condition, $P[N_b = n]$ in (9b) is calculated by ${}_N C_n\, p_b^N (1 - p_b)^{N-n}$.

We plot $S(\alpha)\,C_r(\alpha)$ in Fig. 19. In this figure, $S(\alpha)\,C_r(\alpha)$ is maximized when $\alpha = -0.1$.

As was mentioned in 3.1, the number of sensor nodes N and the ratio of sensing range to radio transmission range may affect the optimal value of α. We thus evaluate two additional cases:

- $N = 400$ and sensing range is not changed (that is, remains 60 m), and
- $N = 400$ and sensing range is changed to 30 m.

The plots of $S(\alpha)C_r(\alpha)$ for these cases are shown in Figs. 20 and 21. From these figures, we can confirm that the optimal value of α is still -0.1.

6. Conclusion

In this paper, we have investigated how forms of stochastic node placement affect the fault tolerance of a sensor network.

To increase tolerance of failure, we must raise the probability of having sensor nodes within sensing range of each target, and of at least one of these nodes having routes to the base station. However, neither of the two most typical forms of stochastic placement, simple diffusion and constant placement, keeps both probabilities high. As a result, both have poor fault tolerance. We have shown that power-law placement, the form proposed in this paper, can raise fault tolerance with an appropriately selected control parameter. In addition, we have shown that power-law placement has superior effectiveness because the sensing-success ratio is almost linearly proportional to the number of nodes.

While we have not proven that power-law placement is the optimal form of stochastic placement, our results clearly indicate that tolerance of both random failures and battery exhaustion can be raised by improving the placement of sensor nodes. Power-law placement with a well-tuned control parameter constitutes good placement.

In further study, we plan to investigate the realization of power-law placement as the superposition of simple diffusion placements in detail.

Acknowledgment

The authors would like to thank Ms. Kyoko Ashitagawa at

Human Resources International Co., Ltd. for her help in performing the simulations.

References

[1] S.J. Lee and M. Gerla, "AODV-BR: Backup routing in ad hoc networks," Proc. 2nd IEEE Wireless Communications and Networking Conf., pp.1311–1316, Sept. 2000.

[2] M.K. Marina and S.R. Das, "On-demand multipath distance vector routing for ad hoc networks," Proc. 9th IEEE Int. Conf. on Network Protocols, pp.14–23, Nov. 2001.

[3] E. Shih, S.H. Cho, N. Ickes, R. Min, A. Sinha, A. Wang, and A. Chandrakasan, "Physical layer driven protocol and algorithm design for energy-efficient wireless sensor networks," Proc. ACM MobiCom'01, pp.272–286, July 2001.

[4] A. Woo and D. Culler, "A transmission control scheme for media access in sensor networks," Proc. ACM MobiCom'01, pp.221–235, July 2001.

[5] K. Sohrabi, J. Gao, V. Ailawadhi, and G.J. Pottie, "Protocols for self-organization of a wireless sensor network," IEEE Pers. Commun., vol.7, no.5, pp.16–27, Oct. 2000.

[6] W.R. Heinzelman, J. Kulik, and H. Balakrishnan, "Adaptive protocols for information dissemination in wireless sensor networks," Proc. ACM MobiCom'99, pp.174–185, Aug. 1999.

[7] W.R. Heinzelman, A. Chandrakasan, and H. Balakrishnan, "Energy-efficient communication protocol for wireless microsensor networks," Proc. IEEE Hawaii Int'l Conf. Sys. Sci., pp.3005–3014, Jan. 2000.

[8] L. Li and Y. Halpern, "Minimum-energy mobile wireless networks revisited," Proc. ICC'01, pp.278–283, June 2001.

[9] H. Saito and H. Minami, "Performance issues and network design for sensor networks," IEICE Trans. Commun., vol.E87-B, no.2, pp.294–301, Feb. 2004.

[10] G. Hoblos, M. Staroswiecki, and A. Aitouche, "Optimal design of fault tolerant sensor networks," Proc. IEEE Int'l Conf. Cont. Apps., pp.462–472, Sept. 2000.

[11] M. Bhardwaj, T. Garnett, and P. Chandrakasan, "Upper bounds on the lifetime of sensor networks," Proc. ICC'01, pp.785–790, June 2001.

[12] A.-L. Barabasi, LINKED: The New Science of Networks, Perseus Publishing, 2002.

[13] I. Daubechies, Ten Lectures on Wavelets, CBMS-NSF Regional Confefence Series in Applied Mathematics, Society of Industrial and Applied Mathematics, 1992.

[14] B. Delyon, A. Juditsky, and A. Benveniste, "Accuracy analysis for wavelet approximations," IEEE Trans. Neural Netw., vol.6, no.2, pp.332–348, March 1995.

[15] C. Intangonwiwat, R. Govindan, and D. Estrin, "Directed diffusion: A scalable and robust communication paradigm for sensor networks," Proc. ACM MobiCom'00, pp.56–67, Aug. 2000.

[16] C. Intangonwiwat, D. Estrin, and R. Govindan, "Impact of network density on data aggregation in wireless sensor networks," Proc. ICDCS'02, pp.1567–1576, July 2002.

Mika Ishizuka graduated from Keio University, Tokyo, with B.E. and M.E. degrees in Control Engineering in 1992 and 1994, respectively. In 1994, she joined NTT and has been engaged in research on traffic control in computer networks. She received the IEICE Information Networks Research Award in 2003. Ms. Ishizuka is a member of the Operations Research Society of Japan.

Masaki Aida received his B.S. and M.S. in Theoretical Physics from St. Paul's University, Tokyo, Japan, in 1987 and 1989, and received the Ph.D. in Telecommunication Engineering from the University of Tokyo, Japan, in 1999. Since joining NTT Laboratories in 1989, he has been mainly engaged in research on traffic issues in ATM networks and computer communication networks. From March 1998 to March 2001, he was a manager at Traffic Research Center, NTT Advanced Technology Corporation (NTT-AT). He is currently a Senior Research Engineer at NTT Information Sharing Platform Laboratories. His current interests include traffic issues in communication systems. He received IEICE's Young Investigators Award in 1996, and Information Networks Research Awards in 2001, 2002, 2003, and 2004. Dr. Aida is a member of the IEEE and the Operations Research Society of Japan.